J. Biochem. **140**, 87–93 (2006)
doi:10.1093/jb/mvj131

Comparative Biochemical Study of *N*-Linked Glycans from Skin of a Squid, *Todarodes pacificus*

Shunji Natsuka[1,2,*], Miwa Ishida[2], Akira Ichikawa[2], Koji Ikura[2] and Sumihiro Hase[1]
[1]*Department of Chemistry, Graduate School of Science, Osaka University, Toyonaka, Osaka 560-0043; and*
[2]*Department of Applied Biology, Kyoto Institute of Technology, Sakyo, Kyoto 606-8585*

Received April 18, 2006; accepted May 18, 2006

For comparative biochemical interest, we analyzed the structures of *N*-glycans in a squid belonging to the Lophotrochozoa, one of the protostome clades. *N*-Glycans were prepared from squid skin by hydrazinolysis and re-*N*-acetylation followed by fluorescent tagging with 2-aminopyridine. The labeled *N*-glycans were purified, and their structures were determined by the two-dimensional HPLC mapping method combined with glycosidase digestions and mass spectrometry. We found that high mannose-type glycans, paucimannose-type glycans and complex-type glycans with a type-1 structure (Galβ1-3GlcNAc) were dominant in squid skin. The complex-type glycans detected in the squid were similar to those in vertebrates, but have not yet been found in the Ecdysozoa, which is another protostome clade. However, paucimannose-type glycans are commonly found in the Ecdysozoa. Thus, the *N*-glycan structures of the squid belonging to the Lophotrochozoa have features common to those in vertebrates and the Ecdysozoa including insects and nematodes.

Key words: HPLC-mapping, invertebrate, *N*-glycans, phylogeny, squid.

Abbreviations: PA, pyridylamino; HPLC, high performance liquid chromatography; Hex, hexose; HexNAc, *N*-acetylhexosamine.

While some prokaryotes have *N*-linked glycans (*1*), it is *N*-linked glycans synthesized from a common high mannose-type structure which are present in eukaryotes. Whereas *N*-glycans in protozoans are utilized as elements similar to the bricks of a house wall, *N*-glycans in metazoans have acquired structural diversity by an additional biosynthetic pathway. The reason why the structures of *N*-glycans exhibit tremendous diversity has not yet been elucidated. Investigation of this problem is of essential importance in the field of glycobiology, and a comparative study of *N*-glycans between species is one of the basic approaches to reach a solution.

We previously reported that the *N*-glycans in a nematode, *Caenorhabditis elegans*, were very similar to those in insects (*2*). Their glycans are characteristic in core-difucosylated pauci-mannose type and precursor of complex type. This observation coincides with a recent classification in which nematodes and insects are closely related in phylogeny, and belong to the Ecdysozoa (*3*), which is one of the two categories of protostomes. This raises the question of what are the structures of the *N*-glycans in the Lophotrochozoa, which is another protostome clade. In order to answer this question, we analyzed the *N*-glycan structures of the squid *Todarodes pacificus*, which belongs to the Lophotrochozoa.

*To whom correspondence should be addressed at: Department of Chemistry, Graduate School of Science, Osaka University, 1-1 Machikaneyama, Toyonaka, Osaka 560-0043. Tel: +81-6-6850-5381, Fax: +81-6-6850-5382, E-mail: natsuka@chem.sci.osaka-u.ac.jp

MATERIALS AND METHODS

Preparation of PA-Glycans from Squid Skin—The skin of a squid, *Todarodes pacificus*, was homogenized in cold acetone using a Polytron homogenizer (Kinematica, Switzerland), followed by lyophilization. Since squid skin contains a lot of extracellular matrix, we chose this tissue for glycan analysis. *N*-Linked glycans were liberated from glycoproteins in the dried delipidized skin by hydrazinolysis as described previously (*4*). Briefly, 2 mg of the sample was heated at 100°C for 10 h with 0.2 ml of anhydrous hydrazine. When the hydrazine had evaporated, *N*-acetylation was initiated with acetic anhydride in a saturated sodium bicarbonate solution. The glycans were passed through a cation exchanger, Dowex 50Wx2 (H^+), to remove sodium ions. The reducing ends of the liberated glycans were tagged with a fluorophore, 2-aminopyridine. Lyophilized samples were heated at 90°C for 60 min with 20 μl of pyridylamination reagent, and were heated at 80°C for 35 min after the addition of 70 μl of reducing reagent, as described elsewhere (*4*). Excess reagents were removed by phenol/chloroform extraction (*5*).

Reducing End Analysis—The PA-glycans were hydrolyzed with 4 M hydrochloric acid at 100°C for 4 h. After complete evaporation of the hydrochloric acid, the liberated monosaccharides were re-*N*-acetylated with acetic anhydride in a saturated sodium bicarbonate solution. PA-monosaccharides derived from reducing ends were purified on a small cation exchange column, as described previously (*6*). Briefly, a sample was applied to a Dowex 50Wx2 (H^+) column (0.5 × 3 cm). After the column had been washed with 2 ml of water, PA-sugars were eluted with 3 ml of a 2.5% ammonia solution. The eluate was lyophilized to

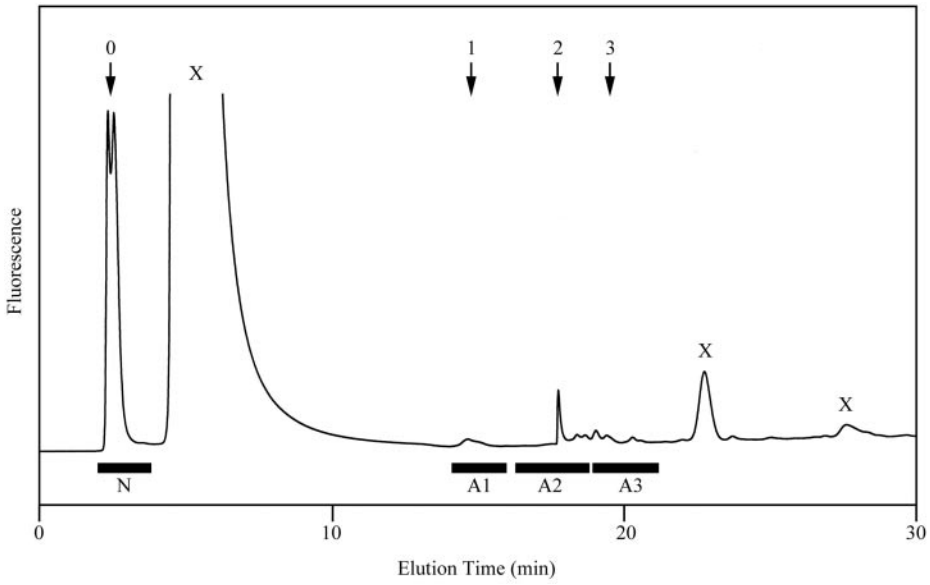

Fig. 1. **Anion-exchange HPLC of PA-glycans from squid.** PA-glycans were separated by DEAE-HPLC. PA-Glycans were fractionated into fractions N, A1, A2 and A3, according to their acidity. Arrows indicate the elution positions of standard *N*-glycans prepared from α1-acid glycoprotein that included the corresponding number of sialic acids. Peaks donated by X did not contain PA-glycans.

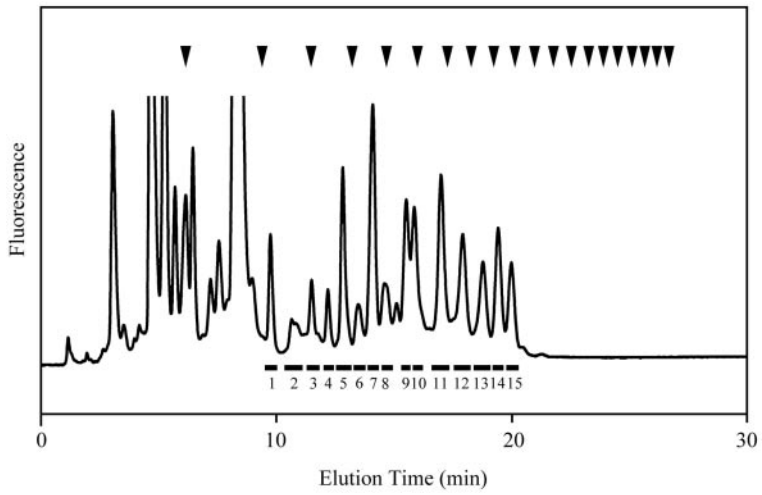

Fig. 2. **Size-fractionation HPLC of the neutral (N) fraction of the squid PA-glycans.** The neutral glycans were separated by size-fractionation HPLC. Ffifteen fractions, of which the molecular sizes were larger than that of isomaltose disaccharide, were isolated. Arrowheads indicate the elution positions of PA-isomaltooligosaccharides of which the degree of polymerization was 1 to 20, from left to right.

remove ammonia, and then analyzed by HPLC (7). PA-sugars were separated on a TSK gel Sugar AX-I column (0.46 × 15 cm) equilibrated with 10% acetonitrile in 0.8 M potassium borate, pH 9.0, at a flow rate of 0.3 ml/min at 74°C, and detected with a fluorescence spectrophotometer at an excitation wavelength of 310 nm and an emission wavelength of 380 nm. The molar ratio of detected GlcNAc in the fractions was taken as the molar ratio of *N*-glycans.

High Performance Liquid Chromatography for PA-Glycan Separation—Size-fractionation HPLC was performed on a TSK gel Amide 80 column (0.46 × 7.5 cm, Tosoh) at a flow rate of 0.5 ml/min. The column was equilibrated with 50 mM ammonium formate, pH 4.4, containing 80% acetonitrile. After a sample had been injected, the acetonitrile concentration was decreased linearly from 80 to 65% in the first 5 min, 65 to 55% in the second 5min, and then 55 to 30% in the next 25 min. The PA-glycans were detected with a fluorescence spectrophotometer at 315 nm excitation and 400 nm emission wavelengths. The molecular size of each PA-glycan is given in terms of glucose units based on the elution times of PA-isomaltooligosaccharides. Reversed phase HPLC was performed on a Cosmosil 5C18-P column (0.2 × 25 cm, Nacalai Tesque) at a flow rate of 0.2 ml/min. The column was equilibrated with 100 mM triethylamine acetate, pH 4.0. After injection of a sample, the 1-butanol concentration was increased linearly from 0.075 to 0.5% in 105 min. The PA-glycans were detected at 315 nm excitation and 400 nm emission wavelengths. The retention time of each PA-glycan was converted to the reversed phase scale as described previously (*8*).

Enzyme Digestion—The PA-glycans were digested with 1 unit/ml of *Arthrobacter ureafaciens* sialidase (Nacalai Tesque, Japan) in 50 mM sodium acetate buffer, pH 5.0, for 20 h at 37°C, 50 units/ml of *E. coli* alkaline phosphatase (Takara Biomedicals, Japan), 1 unit/ml of bovine kidney α-fucosidase (Sigma) in 100 mM sodium phosphate buffer, pH 5.5, for 20 h at 37°C, 10 units/ml of jack bean α-mannosidase (Seikagaku Kogyo, Japan) in 50 mM sodium citrate buffer, pH 4.5, for 20 h at 37°C, 25 units/ml of jack bean β-galactosidase (Seikagaku Kogyo) in 50 mM sodium citrate buffer, pH 3.5, for 20 h at 37°C,

0.2 milliunit/ml of *Streptomyces* lacto-*N*-biosidase (Takara Biomedicals) in 40 mM sodium acetate, pH 5.5, for 16 h at 37°C, 35 units/ml of rice α-glucosidase (Sigma) in 75 mM sodium acetate, pH 4.0, for 12 h at 37°C, or 2.5 units/ml of jack bean β-*N*-acetylhexosaminidase (Seikagaku Kogyo) in 100 mM sodium citrate buffer, pH 5.0, for 20 h at 37°C.

Mass Spectrometric Analysis—PA-Glycans were co-crystallized in a matrix of 2,5-dihydroxybenzoic acid. Mass spectra were recorded using a Voyager-DE-RP BioSpectrometry Workstation (Perseptive Biosystems, MA) with delayed extraction in the reflector mode.

RESULTS

PA-Glycans prepared from squid skin were separated by anion-exchange HPLC (Fig. 1). They were fractionated into N, A1, A2 and A3 according to differences in acidity. Reducing end analysis showed that 86.7% of the *N*-glycans was contained in fraction N, and 3.8%, 4.9%, and 4.6% of them were in fractions A1–A3, respectively. Acidic fractions A1–A3 were resistant to sialidase and alkaline phosphatase digestion (data not shown). Then, fraction N was separated further by size-fractionation HPLC (Fig. 2). Fifteen peaks larger than that of PA-isomaltose were collected. The elution position of PA-isomaltose is indicated by the arrowhead second from the left in Fig. 2. These peaks were further separated by reversed phase HPLC (Fig. 3), and a two-dimensional HPLC map was constructed from their elution positions (Fig. 4).

On comparison of the positions of the peaks on the map to those of standard PA-oligosaccharides, the PA-glycans, i.e., N1, N2, N4, N6, N7, N8, N9, N11, N12, N14, N15, N16, N17, and N18, were assigned to GN2F6, M1A, M2B, M3B, AG1, M3BF6, M4B or M4C, M5A, M6B, M7A, M7B, M8A, M9A, and G1M9A, respectively (Figs. 4 and 5). We could not distinguish the two isomers of M4, corresponding to N9 on the map, since M4B and M4C were eluted very closely even on reversed phase HPLC.

The assignments based on the two-dimensional HPLC map were supported by the results of enzymatic digestion. Bovine kidney α-fucosidase digestion shifted the elution positions of N1 and N8 to the same positions as GN2 and M3B, respectively (data not shown). Jack bean α-mannosidase digestion altered the elution positions of N4, N6, N9, N11, N12, N14, N15, N16, and N17 to the same position as M1A (data not shown). Rice α-glucosidase digested N18 was eluted at the same position as M9A (data not shown). The structures of N3 and N5 were estimated as those of M1AF6 and M2BF6, respectively, since they shifted to the same positions as M1A and M2B on α-fucosidase digestion (data not shown). The results of mass spectrometric analysis also corresponded with the assignment based on the two-dimensional HPLC map (Table 1). The compositions estimated from the observed mass numbers were deoxyHex$_1$HexNAc$_2$, deoxyHex$_1$Hex$_1$HexNAc$_2$, Hex$_2$HexNAc$_2$, deoxyHex$_1$Hex$_2$HexNAc$_2$, Hex$_3$HexNAc$_3$, deoxyHex$_1$Hex$_3$HexNAc$_2$, Hex$_4$HexNAc$_2$, Hex$_5$HexNAc$_2$, Hex$_6$HexNAc$_2$, Hex$_8$HexNAc$_2$, Hex$_9$HexNAc$_2$, and Hex$_{10}$HexNAc$_2$ for N1, N3, N4, N5, N7, N8, N9, N11, N12, N16, N17, and N18, respectively. The mass numbers of N2, N6, N14 and N15 could not be determined, because of their low amounts.

The compositions of N10 and N13 were estimated to be deoxyHex$_1$Hex$_4$HexNAc$_3$ and deoxyHex$_1$Hex$_5$HexNAc$_4$, respectively, by mass analysis. They corresponded to

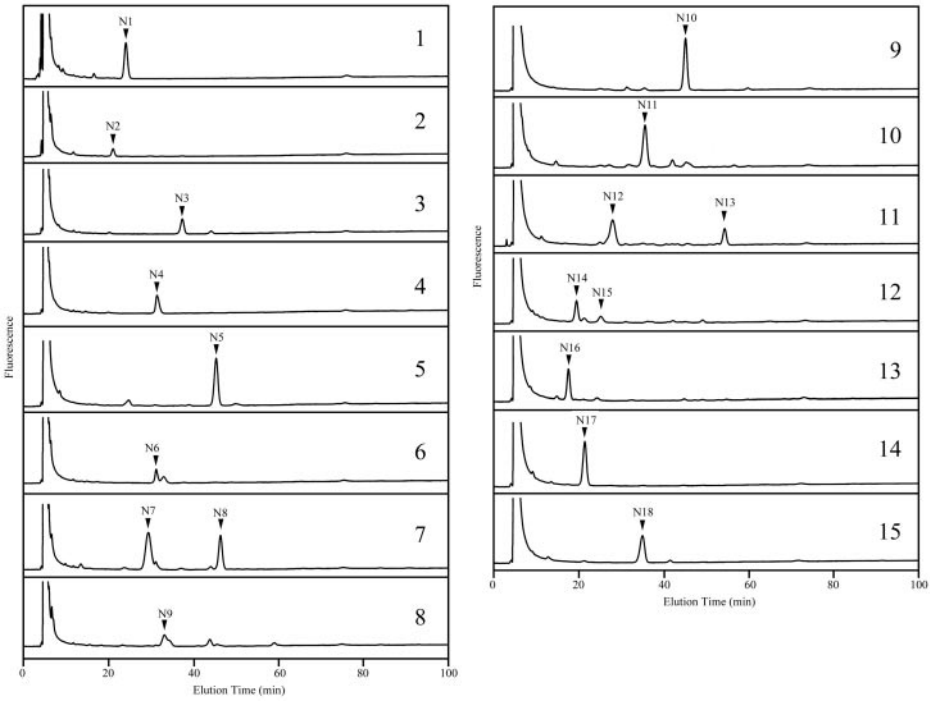

Fig. 3. **Reversed phase HPLC of fractions 1 to 15.** Fractions 1 to 15 obtained on size fractionation HPLC were further separated by reversed phase HPLC, and the major PA-glycans isolated were named N1 to N18.

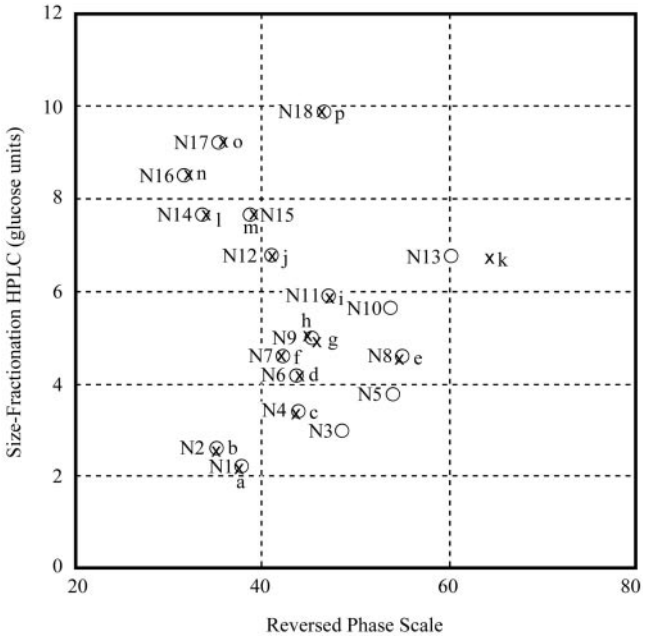

Fig. 4. **Two-dimensional HPLC map of the PA-glycans from squid.** The retention times on size-fractionation and reversed phase HPLC were converted to glucose units and the reversed phase scale, respectively, as described under "MATERIALS AND METHODS." N1 to N18 were plotted on a two-dimensional map as circles. The positions of standard PA-glycans, a to p, are indicated by crosses. The standards were: a, GN2F6; b, M1A; c, M2B; d, M3B; e, M3BF6; f, AG1; g, M4C; h, M4B; i, M5A; j, M6B; k, BIF6; l, M7A; m, M7B; n, M8A; o, M9A; p, G1M9A. The structures of the standard PA-glycans are shown in Table 1 and the text.

Table 1. **Mass analysis of PA-glycans from *T. pacificus*.**

Fraction	Mass (observed)	Mass (expected)	Estimated composition
N1	649.22	648.83 (H^+)	deoxyHex$_1$HexNAc$_2$-PA
	671.26	669.94 (Na^+)	
	687.05	685.88 (K^+)	
N3	849.15	848.02 (K^+)	deoxyHex$_1$Hex$_1$HexNAc$_2$-PA
N4	827.02	826.97 (H^+)	Hex$_2$HexNAc$_2$-PA
	849.28	848.08 (Na^+)	
	865.28	864.02 (K^+)	
N5	973.08	973.12 (H^+)	deoxyHex$_1$Hex$_2$HexNAc$_2$-PA
	995.41	994.23 (Na^+)	
	1,011.35	1,010.17 (K^+)	
N7	1,214.24	1,213.42 (Na^+)	Hex$_3$HexNAc$_3$-PA
	1,230.17	1,229.36 (K^+)	
N8	1,157.35	1,156.36 (Na^+)	deoxyHex$_1$Hex$_3$HexNAc$_2$-PA
	1,173.19	1,172.31 (K^+)	
N9	1,173.13	1,171.87 (Na^+)	Hex$_4$HexNAc$_2$-PA
N10	1,522.07	1,521.71 (Na^+)	deoxyHex$_1$Hex$_4$HexNAc$_3$-PA
	1,537.93	1,537.65 (K^+)	
N11	1,312.86	1,313.41 (H^+)	Hex$_5$HexNAc$_2$-PA
	1,335.03	1,334.52 (Na^+)	
	1,350.94	1,350.46 (K^+)	
N12	1,475.80	1,475.55 (H^+)	Hex$_6$HexNAc$_2$-PA
	1,497.35	1,496.66 (Na^+)	
	1,513.38	1,512.60 (K^+)	
N13	1,888.45	1,887.05 (Na^+)	deoxyHex$_1$Hex$_5$HexNAc$_4$-PA
	1,904.48	1,902.99 (K^+)	
N16	1,799.44	1,798.25 (H^+)	Hex$_8$HexNAc$_2$-PA
N17	1,983.31	1,983.10 (Na^+)	Hex$_9$HexNAc$_2$-PA
	1,999.35	1,999.04 (K^+)	
N18	2,124.85	2,124.13 (H^+)	Hex$_{10}$HexNAc$_2$-PA

fucosylmonoantennary and fucosylbiantennary (BIF6) complex-type *N*-glycans. However, the position of N13 on the HPLC-map did not coincide with that of the standard PA-sugar chain BIF6, of which the structure is Galβ1-4GlcNAcβ1-2Manα1-3(Galβ1-4GlcNAcβ1-2Manα1-6)Manβ1- 4GlcNAcβ1-4(Fucα1-6)GlcNAc-PA (Fig. 4). In order to determine the detailed structures of N10 and N13, enzyme digestion assays were performed. Alpha-fucosidase digestion removed an α-fucose residue from both N10 and N13 (data not shown). Sequential digestion with β-galactosidase and β-*N*-acetylhexosaminidase shifted the elution positions of N10 and N13 to the same position as that of M3BF6 (Fig. 6A). In these digestions, N10 lost a β-galactoside and a β-*N*-acetylglucosaminide, and N13 lost two β-galactosides and two β-*N*-acetylglucosaminides. Lacto-*N*-biosidase digestion also changed the elution positions of N10 and N13 to that of M3BF6, through the removal of one or two Galβ1-3GlcNAc moieties, respectively (Fig. 6B). The structures of N10 and N13 were determined to be those of fucosylmonoantennary and fucosylbiantennary complex-type *N*-glycans with a type I core, respectively (the structures are shown in Table 1). In order to determine the branching structure of N10, additional sequential digestion was performed. Sequential digestion with β-galactosidase and α-fucosidase shifted the elution position of N10 to that of AG1 [GlcNAcβ1-2Manα1-3(Manα1-6)Manβ1-4GlcNAcβ1-4GlcNAc-PA], and not that of AG2 [Manα1-3(GlcNAcβ1-2Manα1-6)Manβ1-4GlcNAcβ1-4GlcNAc-PA] (Fig. 6C). This result clearly showed that the elongated branch of N10 was on the Manα1-3 residue (Fig. 5).

DISCUSSION

Why are *N*-glycans so diverse? To answer this question, firstly we need to know how diverse the *N*-glycans actually are. Comparative observation of *N*-glycan structures provides basic information on this matter. In this study, we observed that the major *N*-glycans in the squid *Todarodes pacificus* could be roughly classified into three types, *i.e.*, high mannose-, paucimannose- and complex-types. The squid high mannose-type glycans had the same isomeric structures as in other animals, including *C. elegans* (*2*, *9*), insects (*10*), and many mammals. All metazoans may have the same isomers of high mannose-type glycans. This indicates that the processing pathway for the high mannose-type glycans may be conserved during the evolutionary process. This conservation may be due to some physiological significance of these particular isomers of high mannose-type glycans. Paucimannose-type glycans are common in invertebrates, whereas there have been few reports of their existence in vertebrates. One of the exceptions is quail ovomucoid, which has M3B as a major component (*11*). Squid skin also included paucimannose-type glycans as major components, among which M2BF6, M1AF6 and GN2F6 were dominant. In particular, the

Peak number	Structure	Abbreviation	Ratio
N1		GN2F6	65
N2		M1A	11
N3		M1AF6	29
N4	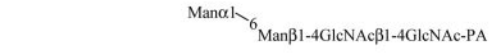	M2B	35
N5	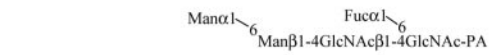	M2BF6	100
N6	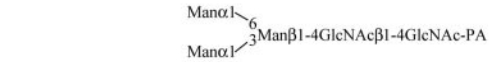	M3B	16
N7	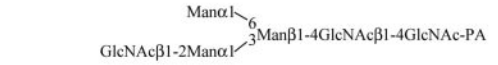	AG1	93
N8	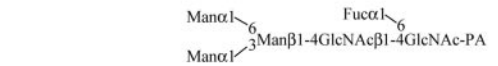	M3BF6	67
N9	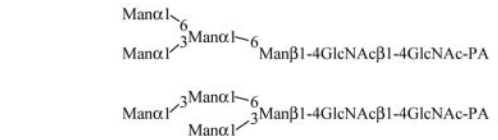	M4B or M4C	16
N10	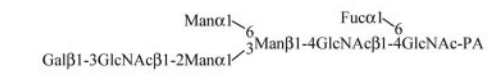	MO1(G3)F6	99
N11	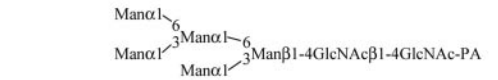	M5A	97
N12	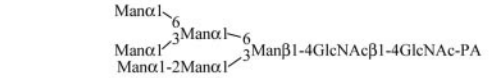	M6B	76
N13	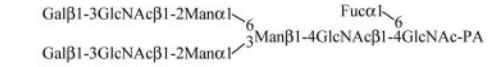	BI(G3)2F6	30
N14	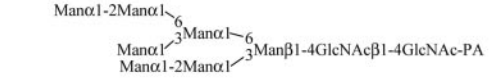	M7A	34
N15	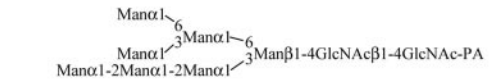	M7B	14
N16	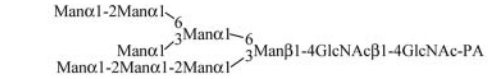	M8A	55
N17	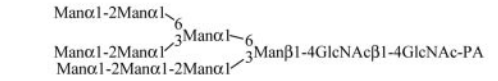	M9A	90
N18	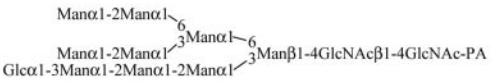	G1M9A	71

Fig. 5. **Proposed structures of neutral *N*-glycans from *T. pacificus*.** The ratio indicates the relative amounts when setting the value of N5 to 100.

short glycan GN2F6 helps distinguish the squid glycans from other reported paucimannose-type glycans. The reason why the paucimannose-type is rare in vertebrates is unknown. The actual content of paucimannose-type glycans in vertebrates is unclear, mainly due to poor recognition of this type of glycan by researchers. The third type of glycans is the complex-type. Vertebrates have, in common, complex-type glycans, consisting of a type II

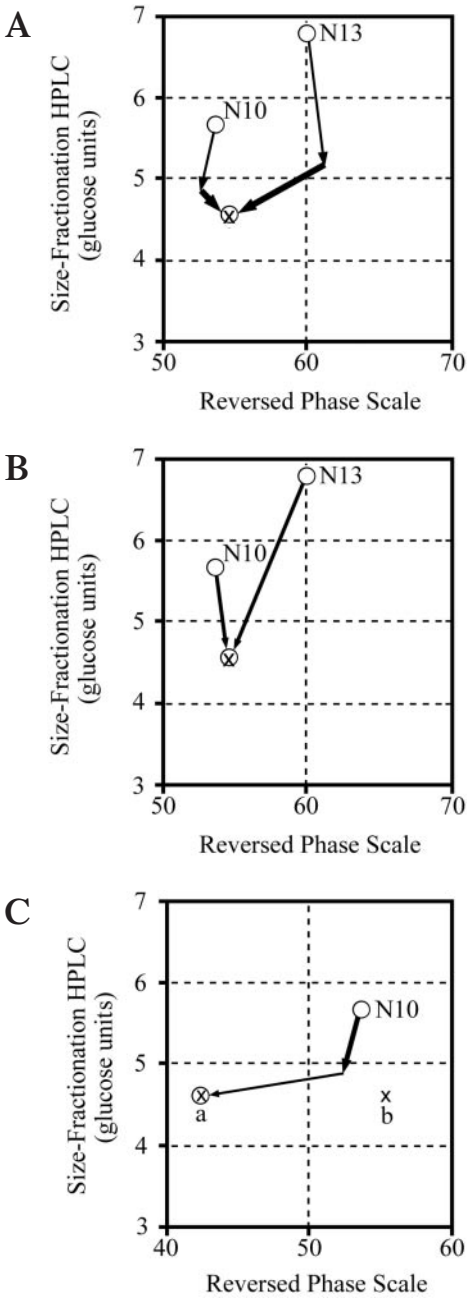

Fig. 6. **Enzyme digestion of PA-glycans from squid.** (A) PA-glycans N10 and N13 were initially digested with β-galactosidase and then with β-*N*-acetylhexosaminidase. The positions of N10 and N13 shifted, as indicated by the arrows. The thin arrows are for β-galactosidase digestion, and the thick ones for β-*N*-acetylhexosaminidase digestion. N10 and N13 moved to the same position on these two digestions. The cross indicates the position of the standard PA-glycan, M3BF6. (B) N10 and N13 were also digested with lacto-*N*-biosidase. The positions of the PA-glycans shifted, as indicated by the arrows. N10 and N13 moved to the same position on the digestion. The cross indicates the position of the standard PA-glycan M3BF6. (C) N10 was initially digested with β-galactosidase, and then with α-fucosidase. The position of N10 shifted, as indicated by the arrows. The thick arrow is for β-galactosidase digestion, and the thin one for α-fucosidase digestion. Crosses a and b indicate the positions of the standard PA-glycans AG1 and AG2, respectively.

backbone (Galβ1-4GlcNAc), but such structures have not been found in invertebrates. Squid skin included complex-type glycans with a type I backbone (Galβ1-3GlcNAc) as one of the major components. A similar core structure has been reported for a glycoprotein in squid (*12*) and octopus (*13*). The type I backbone is also a minor component of vertebrate complex-type glycans, but has not been reported in invertebrates other than cephalopods so far. Consequently, the complex-type glycans of squid are more similar to those in vertebrates, rather than other invertebrates. From the viewpoint of the structure of complex-type glycans, cephalopods, including the squid, are relatively closer to vertebrates than other invertebrates. At present, it is not clear whether this similarity reflects the phylogenetic situation or not. To answer this question, it is necessary to observe the structures of *N*-glycans in many more animal species. Comparative biochemistry research on glycans has only just begun.

This work was supported in part by CREST of Japan Science and Technology Agency (JST) for S.N.

REFERENCES

1. Wacker, M., Linton, D., Hitchen, P.G., Nita-Lazar, M., Haslam, S.M., North, S.J., Panico, M., Morris, H.R., Dell, A., Wren, B.W., and Aebi, M. (2002) *N*-Linked glycosylation in *Campylobacter jejuni* and its functional transfer into *E. coli*. *Science.* **298**, 1790–1793
2. Natsuka, S., Adachi, J., Kawaguchi, M., Nakakita, S., Hase, S., Ichikawa, A., and Ikura, K. (2002) Structural analysis of *N*-linked glycans in *Caenorhabditis elegans*. *J. Biochem.* **131**, 807–813
3. Aguinaldo, A.M., Turbeville, J.M., Linford, L.S., Rivera, M.C., Garey, J.R., Raff, R.A., and Lake, J.A. (1997) Evidence for a clade of nematodes, arthropods and other moulting animals. *Nature* **387**, 489–493
4. Natsuka, S. and Hase, S. (1998) Analysis of *N*- and *O*-glycans by pyridylamination in *Methods in Molecular Biology* (Hounsell, E.F., ed.) Vol. 76, pp. 101–113, Humana Press, Totowa, NJ
5. Natsuka, S., Adachi, J., Kawaguchi, M., Ichikawa, A., and Ikura, K. (2002) Purification method of fluorescence-labeled oligosaccharides by pyridylamination. *Biosci. Biotechnol. Biochem.* **66**, 1174–5
6. Makino, Y., Kuraya, N., Omichi, K., and Hase, S. (1996) Classification of sugar chains of glycoproteins by analyzing reducing end oligosaccharides obtained by partial acid hydrolysis. *Anal. Biochem.* **238**, 54–59
7. Suzuki, J., Kondo, A., Kato, I., Hase, S., and Ikenaka, T. (1991) Analysis by high-performance anion-exchange chromatography of component sugars as their fluorescent pyridylamino derivatives. *Agric. Biol. Chem.* **55**, 283–284
8. Yanagida, K., Ogawa, H., Omichi, K., and Hase, S. (1998) Introduction of a new scale into reversed-phase high-performance liquid chromatography of pyridylamino sugar chains for structural assignment. *J. Chromatogr. A* **800**, 187–198
9. Guerardel, Y., Balanzino, L., Maes, E., Leroy, Y., Coddeville, B., Oriol, R., and Strecker, G. (2001) The nematode *Caenorhabditis elegans* synthesizes unusual *O*-linked glycans: Identification of glucose-substituted mucin-type *O*-glycans and short chondroitin-like oligosaccharides. *Biochem. J.* **357**, 167–182
10. Altmann, F., Staudacher, E., Wilson, I.B.H., and Marz, L. (1999) Insect cells as hosts for the expression of recombinant glycoproteins. *Glycoconj. J.* **16**, 109–123

11. Hase, S., Okawa, K., and Ikenaka T. (1982) Identification of the trimannosyl-chitobiose structure in sugar moieties of Japanese quail ovomucoid. *J. Biochem.* **91**, 735–737
12. Takahashi, N., Masuda, K., Hiraki, K., Yoshihara, K., Huang, H.H., Khoo, K.H., and Kato, K. (2003) *N*-Glycan structures of squid rhodopsin. *Eur. J. Biochem.* **270**, 2627–2632
13. Zhang, Y., Iwasa, T., Tsuda, M., Kobata, A., and Takasaki, S. (1997) A novel monoantennary complex-type sugar chain found in octopus rhodopsin: occurrence of the Galβ1→4Fuc group linked to the proximal *N*-acetylglucosamine residue of the trimannosyl core. *Glycobiology* **7**, 1153–1158